

## Supporting Information

### **Nanoengineered Neutrophil as $^{19}\text{F}$ -MRI Tracer for Alert Diagnosis and Severity Assessment of Acute Lung Injury**

*Sha Li<sup>a,b,+</sup>, Lei Zhang<sup>a,b,+</sup>, Qiuyi Xu<sup>a,b</sup>, Meiju Sui<sup>a,b</sup>, Long Xiao<sup>a,b</sup>, Daiqin Chen<sup>a,b</sup>, Zhong-Xing Jiang<sup>a,b</sup>, Xin Zhou<sup>a,b,c\*</sup>, Shizhen Chen<sup>a,b,c\*</sup>*

<sup>a</sup> State Key Laboratory of Magnetic Resonance and Atomic and Molecular Physics, National Center for Magnetic Resonance in Wuhan, Wuhan Institute of Physics and Mathematics, Innovation Academy for Precision Measurement Science and Technology, Chinese Academy of Sciences-Wuhan National Laboratory for Optoelectronics, Huazhong University of Science and Technology, Wuhan, 430071, China.

<sup>b</sup> University of Chinese Academy of Sciences, Beijing 100049, China.

<sup>c</sup> School of Biomedical Engineering, Hainan University, Haikou, 570228, China.

Corresponding author: [chenshizhen@wipm.ac.cn](mailto:chenshizhen@wipm.ac.cn); [xinzhou@wipm.ac.cn](mailto:xinzhou@wipm.ac.cn).

<sup>+</sup> These authors contributed equally to this work

Keywords:  $^{19}\text{F}$ -MRI, nanoengineered neutrophil, perfluorocarbon, acute lung injury, diagnosis

## Materials

Perfluoro-15-crown-5-ether (PFCE, C<sub>10</sub>F<sub>20</sub>O<sub>5</sub>) was purchased from Tokyo Chemical Industry Co., Ltd. Purified egg lecithin (E80S), 1,2-dioleoyl-3-trimethylammonium-propane (DOTAP) and dioleoyl phosphatidylethanolamine (DOPE) were purchased from Avanti Polar Lipids, Inc. DOPE-Rhodamine B was purchased from Xi'an ruixi Biological Technology Co., Ltd. (Xi'an, China). 1,1'-Dioctadecyl-3,3,3',3'-Tetramethylindodicarbocyanine,4-Chlorobenzenesulfonate Salt (DiD) and 3,3'-dioctadecyloxacarbocyanine perchlorate (DiO) were purchased from Beyotime Biotechnology Co., Ltd. (Shanghai, China). iFluor® 488-Wheat Germ Agglutinin (WGA) was purchased from Xi'an Biolite Biotech Co., Ltd. (Xi'an, China). Lipopolysaccharide (LPS) from *Escherichia coli* 055:B5 and heparin sodium were purchased from Sigma-Aldrich. FITC-conjugated anti-mouse Ly-6G/Ly-6C (Gr-1) antibody, PE-conjugated anti-mouse CD11b antibody, and FITC-conjugated anti-mouse F4/80 antibody were acquired from Biolegend. All reagents were analytical or better grade and used without further purification. All aqueous solution was prepared with ultrapure water (Mill-Q, Millipore, 18.2 MΩ·cm<sup>-1</sup> resistivity).

## Instrumentation

PFCE nanoemulsion was synthesized using a high-pressure homogenizer (NanoGenizer, America). Transmission electron microscope (TEM) images were characterized with a Tecnai G2 F30 TEM (FEI). Energy Dispersive Spectroscopy analysis was taken with Xplore (Oxford). Scanning electron microscope (SEM) images were characterized with a SU8010 SEM (Hitachi). Size and zeta potential of PFCE nanoemulsion were performed by dynamic light scattering (DLS) (Zetasizer Nano ZS, Malvern). Cell fluorescence images were taken by a confocal laser scanning microscope (CLSM) (Nikon A1). Fluorescence intensity was quantified by CytoFLEX S flow cytometry (Beckman). *In vivo* fluorescence imaging experiments were conducted on PerkinElmer IVIS Spectrum. Intravital microscopy imaging of pulmonary microcirculation was performed with an IVIM Technology Intravital Microscope (IVM-CMS3). <sup>19</sup>F nuclear magnetic resonance (NMR) was recorded on a Bruker Ascend WB 500 MHz spectrometer. <sup>1</sup>H and <sup>19</sup>F magnetic resonance imaging (MRI) experiments were performed using a 9.4 T microimaging system (Bruker, Germany).

## Preparation of PFCE nanoemulsion

The PFCE nanoemulsion (PFC-EM) was prepared using a conventional film hydration method according to the previously reported procedure with some modifications.<sup>[1]</sup> Briefly, a mixture of purified egg lecithin (E80S), 1,2-dioleoyl-3-trimethylammonium-propane (DOTAP) and dioleoyl phosphatidylethanolamine (DOPE) at a weight ratio of 45:1:1 was dissolved in anhydrous chloroform and then dried into thin film by rotary evaporation at 45°C under reduced pressure, followed by evaporation under high vacuum overnight. The dried lipid film was then hydrated with deionized water through gentle mixing and stirring. 10% wt/vol PFCE was emulsified into 45 mg/mL lipid mixture by means of sonication for 15 min (30% vibration amplitude with 2 s on/2 s off using an Ultrasonic Homogenizer JY92-IIN). The resulting crude emulsion was subjected to high-pressure homogenization (70 MPa, 10 cycles) to reduce droplet size and promote uniformity. The formed nanoemulsion was filtered through a 0.22 µm sterile filter unit (Guangzhou Jet Bio-Filtration Co., Ltd.). The resulting PFC-EM solution was centrifuged at 3000 rpm for 10 minutes to remove large particulate precipitates. The supernatant solution was stored at 4 °C until use.

For CLSM imaging, DOPE-Rhodamine B (Ex/Em ~560/580 nm) was used as a fluorescent lipid marker to produce PFC-EM/RB. For *in vivo* fluorescence imaging, the PFCE crude emulsion was mixed with 0.1 mg of DiD (Ex/Em ~644/665 nm) at room temperature for 1 hour.

### Characterization of PFC-EM

DLS was used to measure the hydrodynamic diameter and surface charge of PFC-EM. TEM characterized the size and morphology of PFC-EM. Energy dispersive X-ray spectroscopy (EDS) was carried out for elemental analysis. PFC-EM aqueous solution was dropped onto a copper grid and stained with 2% fresh ammonium molybdate.

<sup>19</sup>F content of PFC-EM was measured on a Bruker Ascend WB 500 MHz spectrometer. PFC-EM were dissolved in purified water with 10% D<sub>2</sub>O (Sigma Aldrich). Sodium trifluoromethanesulfonate (CF<sub>3</sub>SO<sub>3</sub>Na, Sigma Aldrich) was added as an internal reference.

<sup>19</sup>F phantom images were acquired on a 9.4 T microimaging system (Bruker, Germany). PFC-EM aqueous solutions with different concentrations (<sup>19</sup>F: 6.25, 12.5, 25, 50, 100 mM) were transferred to 5 mm NMR tubes. Rapid acquisition with relaxation enhancement (RARE) sequence was used and the parameters were as follows: repetition time (TR) = 4000 ms, echo times (TE) = 3 ms, RARE factor = 8, matrix = 32×32, field of view (FOV) = 20×20 mm, slice thickness = 20 mm, number of averages (NA) = 128.

### **Isolation of neutrophils from murine peripheral blood**

A density-gradient centrifugation technique was used on donor whole blood for analysis to obtain a nearly pure preparation of neutrophils.<sup>[2]</sup> LPS (1.5 mg/kg) was injected intraperitoneally into the mice to activate neutrophils *in vivo*. Murine peripheral blood samples were collected in evacuated tube with heparin sodium at a final concentration of 5 IU/mL. Neutrophils were isolated by a murine peripheral blood neutrophil separation kit (Solarbio, Beijing, China). Briefly, blood samples were placed on top of the density gradient centrifugation reagent and centrifuged according to the manufacturer's instructions. After the lysis of residual erythrocytes, the cells were washed three times with cold PBS. The purified neutrophils were cultured in RPMI 1640 medium with 20% fetal bovine serum (FBS, Cell-Box Biological products Trading Co., Ltd.).

### **Characterization of neutrophils**

The neutrophil suspension was treated with Weigert-Giemsa stain (Solarbio). The stained cells were dropped onto the slide, the morphology of neutrophils were observed under the microscope (Nikon ECLIPSE Ci) by using Olympus<sup>TM</sup> 100 X oil immersion objective.

The purity of isolated neutrophils was determined by flow cytometry. Cells were immunofluorescence double stained with PE-conjugated anti-mouse CD11b (250 ng/mL, BioLegend) and FITC-conjugated anti-mouse Ly6G/Ly6C (Gr-1) (250 ng/mL, BioLegend) antibodies for 1 hour.

The trypan blue exclusion test (Solarbio) was used to determine the percentage of viable cells. Cells were suspended in PBS and incubated with 0.4% trypan blue at room temperature for 3-5 min. A drop of the trypan blue/cell mixture was then applied to a hemacytometer (RWD C100-SE) and examined to determine the percentage of cells with clear cytoplasm (viable) versus cells with blue cytoplasm (dead). More than 90% of the survival rate could be considered as efficient sample for subsequent experiments.

The Calcein-AM/PI live/dead cell double staining kit (Beyotime Biotechnology) was utilized to stain live and dead cells simultaneously with fluorescence. Acetoxymethyl ester of calcein cleaved by esterases within live cells produce green fluorescence, while dead cells exhibit red fluorescence.

### **Uptake of PFC-EM by neutrophils *in vitro***

Neutrophils ( $1 \times 10^6$  cells/mL) were incubated with serum-free medium containing 0.1 mg/mL PFC-EM/RB for different times (10, 30, 60, 120 min). To remove the extracellular nanoparticles, the cells were centrifuged at 1200 rpm for 5 min and washed twice with ice-cold PBS, resuspended in PBS and ready for subsequent experiments. The distribution of PFC-EM/RB in neutrophils was detected by CLSM. Neutrophils internalized with PFC-EM/RB were seeded into confocal dishes ( $1 \times 10^5$  cells per dish), incubated with iFluor 488-WGA (10  $\mu$ g/mL) and Hoechst 33342 (10  $\mu$ g/mL) at 37°C for 15 min. Cells were centrifuged at 1200 rpm for 5 min, and washed with ice-cold PBS thrice. Then the green fluorescence of iFluor 488-WGA (Ex/Em = 491/516 nm), red fluorescence of PFC-EM/RB (Ex/Em = 560/580 nm), and blue fluorescence of Hoechst 33342 (Ex/Em = 350/460 nm) were imaged by CLSM.

The cellular uptake efficiency of PFC-EM/RB was detected by flow cytometry via the PE-A channel. Flow cytometry data was analyzed using Flow Jo Software (BD, USA).

In order to quantify the loading amount of PFCE, neutrophils ( $1 \times 10^7$  cells) were incubated with different concentrations of PFC-EM. After purification, Neu@PFC suspension was transferred to a 5 mm NMR tube, and  $\text{CF}_3\text{SO}_3\text{Na}$  was added as an internal standard. The content of PFCE was calculated from the integral area ratio of the  $^{19}\text{F}$ -NMR peaks at -78.7 ppm (C-F of  $\text{CF}_3\text{SO}_3\text{Na}$ , set as 1.0) and -91.9 ppm (C-F of PFCE).

### Cell viability

The neutrophils were seeded in a 96-well culture plate at a density of  $1 \times 10^4$  per well. Then, the cells were incubated with PFC-EM at different concentrations in 5%  $\text{CO}_2$  at 37°C for 1 hour. After the cell media was removed, 10  $\mu$ L of CCK-8 solution (2.5 mg/mL in PBS, Beyotime Biotechnology) and 90  $\mu$ L of culture medium was added into each well, followed by incubating for another 1 hour. Later, the absorbance was measured on a microplate reader (Spectra MAX 190) at the wavelength of 450 nm. The relative cell viability was calculated as  $(A_t - A_{nc}) / (A_{pc} - A_{nc}) \times 100\%$ , where  $A_t$ ,  $A_{pc}$ , and  $A_{nc}$  indicate the absorbance of tested groups, positive, and negative controls, respectively.

### Physiological functions of Neu@PFC

The physiological activities of Neu@PFC were evaluated, including the inflammation-responsive expression of the specific protein CD11b and chemotaxis behavior. To evaluate inflammation-induced CD11b expression, the prepared neutrophils and Neu@PFC were incubated with different concentrations of fMLP (0, 1, 10, 100 nM) at 37°C for 30 min, rinsed

three times with ice-cold PBS, and immunostained with PE-conjugated anti-mouse CD11b antibody (250 ng/mL) for 1 hour. After thorough rinsing with ice-cold PBS, CD11b immunoexpression was determined using a flow cytometry to measure PE fluorescence intensity.

The chemotaxis of Neu@PFC was evaluated using a transwell migration assay. Cell culture inserts were put into the 24-well cell plate (polycarbonate membrane, 3.0  $\mu\text{m}$  pore size, 6.4 mm membrane diameter, 0.33  $\text{cm}^2$  surface area, Guangzhou Jet Bio-Filtration Co., Ltd.). The prepared neutrophils and Neu@PFC were suspended in 100  $\mu\text{L}$  FBS-free culture medium and added into the upper well. The bottom well was filled with 600  $\mu\text{L}$  medium containing various concentrations of fMLP (0, 1, 10, 100 nM) as a chemoattractant. After 1 hour incubation at 37°C, cell culture inserts were removed. The cell count in the bottom well was determined using an automated cell counter (RWD C100-SE). In addition, cells reaching the bottom well were stained with crystal violet (Solarbio) and imaged using the Olympus<sup>TM</sup> 100 X oil immersion objective.

### **RNA sequencing and data analysis**

A total amount of 1  $\mu\text{g}$  RNA per sample was used as input material for the RNA sample preparations. Sequencing libraries were generated using VAHTSTM mRNA-seq V2 Library Prep Kit for Illumina<sup>®</sup> following manufacturer's recommendations and index codes were added to attribute sequences to each sample. Briefly, mRNA was purified from total RNA using poly-T oligo-attached magnetic beads. Fragmentation was carried out using divalent cations under elevated temperature in VAHTSTM First Strand Synthesis Reaction Buffer (5X). First strand cDNA was synthesized using random hexamer primer and M-MuLV Reverse Transcriptase (RNase H-). Second strand cDNA synthesis was subsequently performed using DNA polymerase I and RNase H. Remaining overhangs were converted into blunt ends via exonuclease/polymerase activities. After adenylation of 3' ends of DNA fragments, adaptor was ligated to prepare for library. In order to select cDNA fragments of preferentially 150~200 bp in length, the library fragments were purified with AMPure XP system (Beckman Coulter, Beverly, USA). Then 3  $\mu\text{L}$  USER Enzyme (NEB, USA) was used with size-selected, adaptor-ligated cDNA at 37 °C for 15 min followed by 5 min at 95 °C before PCR. Then PCR was performed with Phusion High-Fidelity DNA polymerase, Universal PCR primers and Index (X) Primer. At last, PCR products were purified (AMPure XP system) and library quality was assessed on the Agilent Bioanalyzer 2100 system. The

libraries were then quantified and pooled. Paired-end sequencing of the library was performed on the NovaSeq sequencers (Illumina, San Diego, CA).

After data assessment and quality control, paired-end clean reads were aligned to the reference genome using Hisat2 v2.0 and BEDTools v2.26.0 was used to statistical analysis the gene coverage ratio. And then TPM of each gene was calculated by StringTie (version 1.3.3b). Differential expression analysis of two groups was performed using the DESeq2 R package (v1.12.4). Genes with  $P < 0.05$  and fold change  $> 1.5$  or  $< 2/3$  found by DESeq2 were assigned as differentially expressed. In addition, GO (Gene Ontology) analysis of differentially upregulated genes in the fMLP group compared with the PBS group was performed by clusterProfiler R package (v3.0.5). GO terms with  $q < 0.025$ , rich factor  $\geq 0.15$ , annotated gene number  $\geq 20$  and significant gene number  $\geq 15$  were assigned as significantly enriched in the gene list. Then GO terms including “chemokine”, “chemotaxis”, “interleukin-1 beta”, “interleukin-6”, “interleukin-8”, “inflammatory”, “neutrophil”, “tumor necrosis factor” were visualized. All results were visualize with R (version 4.3.1).

### **Animal experiments**

Male Balb/c mice (8-10 weeks old) weighing approximately 25 g were purchased from the Vital River Laboratory Animal Technology Co. Ltd. (Beijing, China). The mice were housed under specific pathogen-free (SPF) conditions and in a standard light-dark cycle with free access to food and water. According to the Guide for Care and Use of Laboratory Animals, animals were housed and treated. All animal experiments in this study were approved by the Ethics Committee for Animal Research, Innovation Academy for Precision Measurement Science and Technology, Chinese Academy of Sciences.

### **LPS-induced acute lung injury (ALI) mouse model**

LPS was dissolved at 6 mg/mL in sterile PBS and diluted to the concentrations for the individual experiments. Prior to ALI modeling, mice were anesthetized by intraperitoneal injection of 10% ethyl urethane and 2% chloral hydrate (8 mL/kg body weight). A 22-gauge catheter was inserted into the trachea under direct visualization. The LPS solution (6  $\mu\text{g/g}$ , 100  $\mu\text{L}$ ) was gently introduced at the distal end of the catheter. To avoid volume-induced lung damage, no pressure was applied during the instillation of LPS. Instead, the solution was introduced by spontaneous respiration of the mice. Following administration, animals were recovered on a heating pad and observed for signs of respiratory distress. ALI mice were

sacrificed at the following time points: 3, 6, 12, and 24 hours. The lungs were harvested, fixed in 4% paraformaldehyde, embedded in paraffin, and cut into 4  $\mu\text{m}$ -thick slices. Hematoxylin and eosin (H&E) staining was performed according to the manufacturer's protocol. Lung sections were further immunofluorescence stained with PE-conjugated anti-mouse Ly6G and FITC-conjugated anti-mouse F4/80 antibodies to label neutrophils and macrophages, respectively.

To verify the neutrophil's infiltration toward ALI of varying severity. Mice were randomized to receive either 100  $\mu\text{L}$  LPS at doses of 0.08, 0.4, 1.6, 6  $\mu\text{g/g}$ , or 100  $\mu\text{L}$  PBS as control. After 12 hours, blood samples were obtained from the retro-orbital plexus and collected in an EDTA tube. Serum was separated from blood following an period of 30 min at room temperature, and samples were centrifuged at 2,000 $\times$ g for 30 min to remove cells and debris. Following, clarified serum was transferred to a new tube and stored at -80  $^{\circ}\text{C}$  until use. Bronchoalveolar lavage fluid (BALF) was collected with three serial instillations of sterile PBS (0.6 mL) through the tracheostomy. Centrifuge the BALF samples at 800 $\times$ g at 4 $^{\circ}\text{C}$  for 10 min, supernatants were separately frozen (-80  $^{\circ}\text{C}$ ) for further analysis. The expression levels of the inflammatory cytokines interleukin-6 (IL-6), interleukin-1 $\beta$  (IL-1 $\beta$ ) and tumor necrosis factor- $\alpha$  (TNF- $\alpha$ ) in serum and BALF were determined by enzyme-linked immunosorbent assay (ELISA, Bioswamp Life Science Lab Co., Ltd.) using specific antibodies and standards according to the manufacturer's instruction. Furthermore, the lungs of ALI mice were harvested and fixed for histological examination by H&E staining and immunofluorescence staining for neutrophils (PE-conjugated anti-mouse Ly6G antibody).

### **Chest CT experiments of ALI mice**

The CT scanning was performed on a Micro-CT (Bruker Sky Scan 1176, Germany) under continuous, inhaled isoflurane anesthesia. The parameters were as follows: wave filter = Al-0.5 mm, X-ray voltage = 50 kV, image resolution = 35  $\mu\text{m}$ .

### ***In vivo* imaging of Neu@PFC in ALI mice through *i.t.* administration**

ALI mice (4 hours after the instillation of LPS) and healthy mice were received *i.t.* administration of Neu/DiO@PFC/DiD and bare PFC-EM/DiD. Mice were anesthetized with isoflurane and imaged by the IVIS Spectrum system at time points of 1, 4, 8, 12, 24 and 48 hours post-administration. The mice were euthanized, and major organs (brain, heart, liver, spleen, lungs, kidneys, and intestine) were harvested and subjected to *ex vivo* imaging.



Fluorescence was detected with 640/20 nm excitation and 680/20 nm emission filters. The lungs were fixed in 4% paraformaldehyde, sectioned and stained with H&E and observed under an optical microscope. The other lung sections were stained with DAPI and observed by CLSM.

For *in vivo* MRI study, ALI mice received *i.t.* administration of Neu@PFC (2  $\mu\text{mol}$  PFCE, 100  $\mu\text{L}$ ) and PFC-EM (2  $\mu\text{mol}$  PFCE, 100  $\mu\text{L}$ ). Mice were anesthetized by intraperitoneal injection of 10% ethyl urethane and 2% chloral hydrate (8 mL/kg body weight). *In vivo*  $^{19}\text{F}$  MRI was performed at different time points (1, 8 and 24 hours post-administration) by using a 9.4 T microimaging system (Bruker, Germany). A reference phantom with PFC-EM aqueous solution ( $^{19}\text{F}$  content: 200 mM) was along with the mouse body for quantification purpose.  $^1\text{H}$  anatomical images were acquired with an axial  $T_2$ -weighted RARE sequence and the parameters: repetition time (TR) = 3500 ms, echo times (TE) = 33 ms, RARE factor = 8, matrix = 256 $\times$ 256, field of view (FOV) = 35 $\times$ 35 mm, slice thickness = 1 mm, number of averages (NA) = 6. Density-weighted  $^{19}\text{F}$ -MRI was implemented with a RARE sequence and the following parameters: repetition time (TR) = 4000 ms, echo times (TE) = 3 ms, RARE factor = 8, matrix = 32 $\times$ 32, field of view (FOV) = 43.2 $\times$ 43.2 mm, slice thickness = 3 mm, number of averages (NA) = 48. The  $^{19}\text{F}$ -MRI images were displayed by pseudocolor processing and overlaid on the corresponding anatomic  $^1\text{H}$ -MRI images.

### ***In vivo* imaging of Neu@PFC in ALI mice through *i.v.* administration**

ALI mice with different dose of LPS instillation (0, 0.08, 0.4, 1.6, 6  $\mu\text{g/g}$ , 100  $\mu\text{L}$ ) were *i.v.* administered with Neu/DiO@PFC/DiD (5.75  $\mu\text{mol}$  PFCE, 100  $\mu\text{L}$ ) and bare PFC-EM/DiD (5.75  $\mu\text{mol}$  PFCE, 100  $\mu\text{L}$ ) through tail vein. After 12 hours, mice were sacrificed, and main organs (lungs, hearts, livers, spleens and kidneys) were harvested and observed using an IVIS spectrum imaging system with a DiD filter (excitation filter 640/20 nm; emission filter 680/20 nm). Region-of-interests were circled the organs, and the fluorescence intensity was analyzed. The lungs were fixed in 4% paraformaldehyde, sectioned and stained with H&E and observed under an optical microscope. The lung sections were further stained with DAPI and observed by CLSM.

For *in vivo* MRI study, 4 hours after the LPS instillation, ALI mice received *i.v.* administration of Neu@PFC (5.75  $\mu\text{mol}$  PFCE, 100  $\mu\text{L}$ ) and PFC-EM (5.75  $\mu\text{mol}$  PFCE, 100  $\mu\text{L}$ ) through tail vein. The mice were anesthetized at 12 hours, MRI was performed with a 9.4 T microimaging system (Bruker, Germany). The parameters of  $^1\text{H}$ -MRI were the same as

those of above *in vivo* MRI experiments.  $^{19}\text{F}$ -MRI was implemented with the following parameters: TR = 4000 ms, TE = 3 ms, RARE factor = 8, matrix =  $32 \times 32$ , FOV =  $43.2 \times 43.2$  mm, slice thickness = 3 mm, NA = 384. The  $^{19}\text{F}$ -MRI images were displayed by pseudocolor processing and overlaid on the corresponding anatomic  $^1\text{H}$ -MRI images. Region of interest (ROI) were circled around the lung area.

### **Intravital pulmonary imaging**

To observe the migration and infiltration of Neu@PFC into lung vessels, intravital microscopy (IVM) imaging of the lung was further obtained using an IVIM Technology Intravital Microscope (IVM-CMS3). Purified neutrophils were stained with DiO, while PFC-EM were stained with Rhodamine-B to prepare double fluorescent labeled Neu/DiO@PFC/RB. The Neu/DiO@PFC/RB were administered via *i.t.* or *i.v.* route to healthy mice as well as ALI mice. Before the direct pulmonary capillary imaging, 200  $\mu\text{L}$  of 2.5 mg/mL evance blue (Solarbio) was injected into the mice via the tail vein as an agent for fluorescence angiography to visualize the vasculature of the lung *in vivo*. Later, the surgical procedure of thoracotomy was performed to expose the lung surface. The minimal negative suction pressure of 20-30 mmHg was applied via a suction tube to minimize the motion-induced interruption during the pulmonary imaging. Intubation and mechanical ventilation with the ventilator were conducted to assist respiration during the pulmonary imaging. DiO labeled neutrophils were imaged by detection range of 503-558 nm, RB labeled PFC-EM were imaged by detection range of 574-626 nm, evance blue labeled lung vasculature was imaged by detection range of 641-708 nm.

### **Biological safety assay**

To estimate the biological safety of Neu@PFC and bare PFC-EM *in vivo*. Neu@PFC and bare PFC-EM were *i.v.* and *i.t.* administered in both healthy and ALI mice. H&E staining was carried out on the major organs (heart, liver, spleen, lungs, kidneys) at 24 hours post-administration. Blood samples were acquired for blood biochemistry, and hematology tests. The BALF and serum samples were collected to quantify IL-6, IL-1 $\beta$ , and TNF- $\alpha$  cytokine concentrations through ELISA kits.

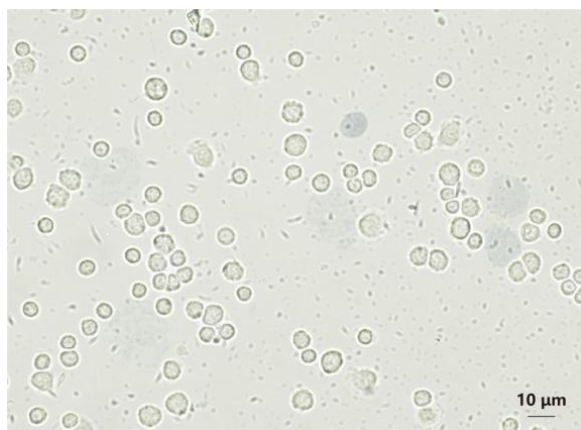


Figure S1. Trypan blue staining of neutrophils. Trypan blue dyes can infiltrate diseased cells with a compromised membrane, resulting in blue cytoplasmic staining. Conversely, viable cells with intact cell membranes are impermeable to trypan blue. Therefore, they retain their original appearance without any staining.

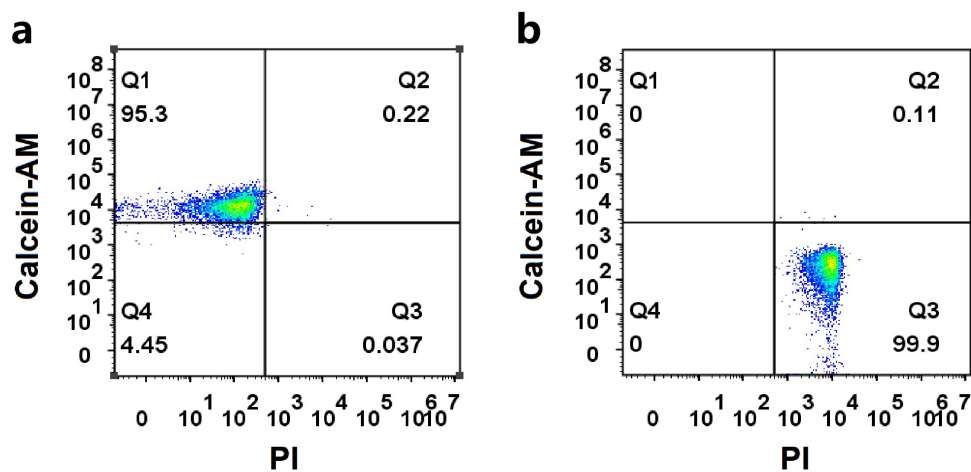


Figure S2. Determination of cell viability by calcein-AM/PI staining and flow cytometry. (a) The prepared neutrophils. (b) Neutrophils were fixed with 4% paraformaldehyde.

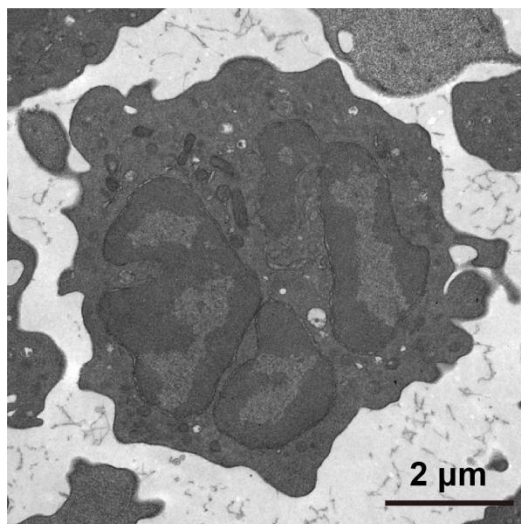


Figure S3. TEM image of the prepared neutrophil. The cell exhibited various granules clearly visible in the cytoplasm, along with a distinct lobulated nucleus.

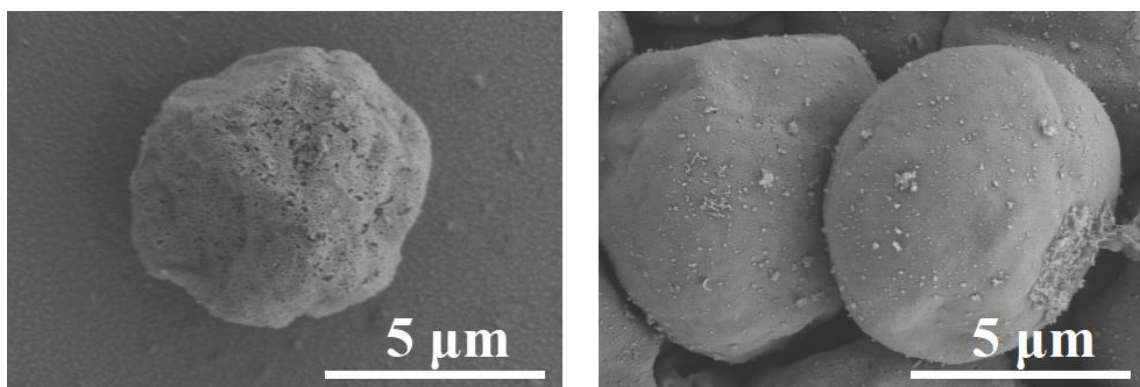


Figure S4. SEM image of the prepared neutrophil (left) and Neu@PFC (right). The unlabeled neutrophil exhibited a round shape, while Neu@PFC revealed electrostatic attraction between the positively charged PFC-EM and the negatively charged cell membrane.

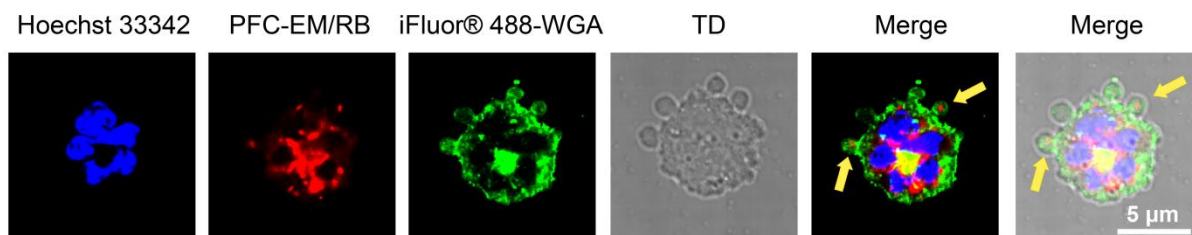


Figure S5. CLSM image of neutrophils incubated with PFC-EM for 2 hours. The nucleus was labeled with Hoechst 33342 (blue). Cell membrane was labeled with iFluor 488-WGA (green). PFC-EM/RB (red) were phagocytized by neutrophil and primarily located in the cytoplasm. The yellow arrow indicates the neutrophil's exocytosis activity.

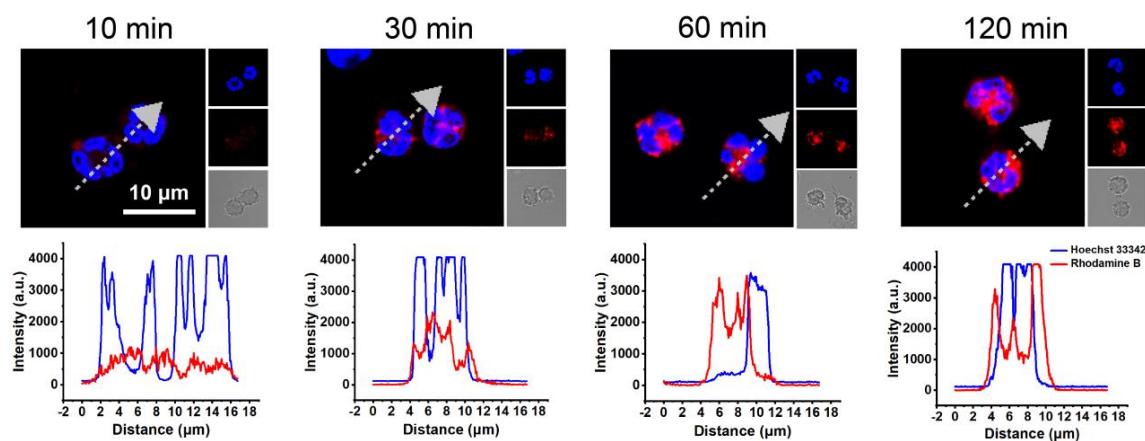


Figure S6. CLSM images (top) and line-scan profiles of fluorescence intensity (bottom) of neutrophils incubated with PFC-EM/RB (red) under 100 nM fMLP for different times (10, 30, 60, and 120 min). Nucleus was labeled with Hoechst 33342 (blue).

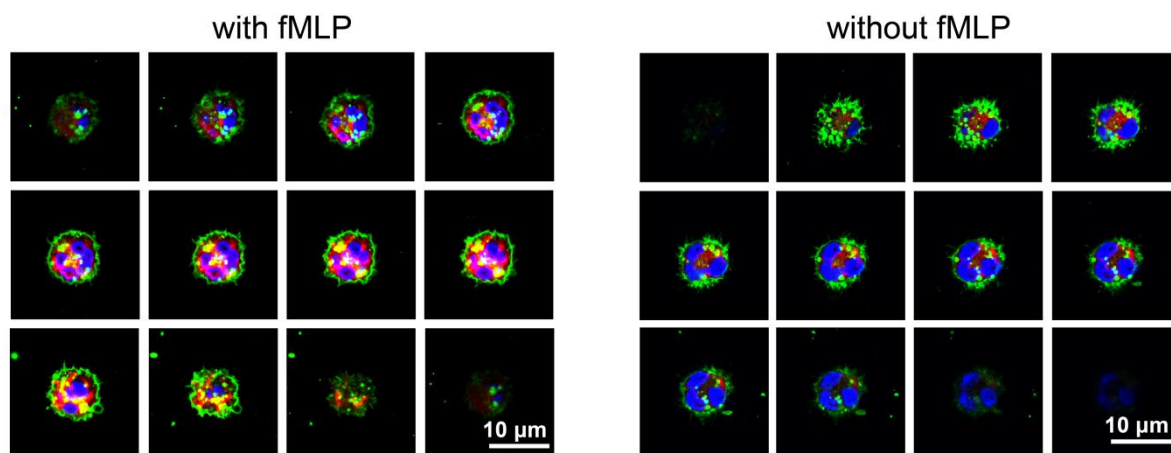


Figure S7. High-resolution CLSM images of neutrophils incubated with PFC-EM/RB (red) in the presence/absence of fMLP activation. Cell nucleus was stained with Hoechst 33342 (blue). Cell membrane was stained with iFluor 488-WGA (green).

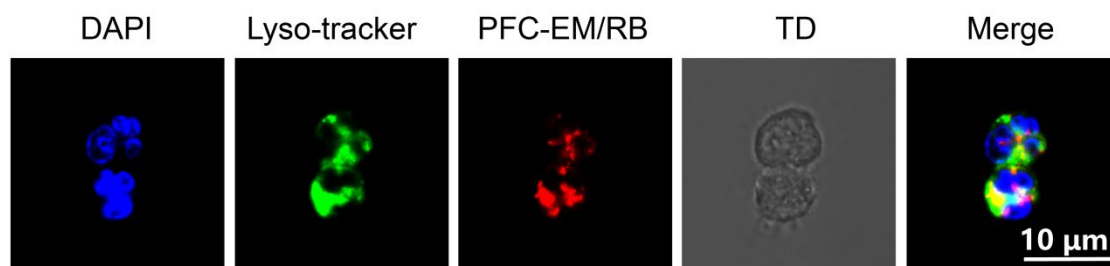
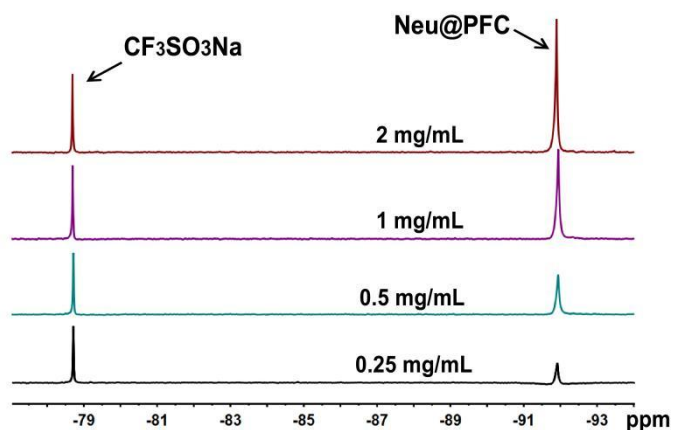


Figure S8. CLSM images demonstrating the localization of PFC-EM/RB within the lysosomes of neutrophil.



PFC-EM Concentration	PFCE/ $10^6$ cell
2 mg/mL	$1.75 \times 10^{-4}$ mmol
1 mg/mL	$1.15 \times 10^{-4}$ mmol
0.5 mg/mL	$6.75 \times 10^{-5}$ mmol
0.25 mg/mL	$2.84 \times 10^{-5}$ mmol

Figure S9.  $^{19}\text{F}$ -NMR spectra of neutrophils incubated with different concentrations of PFC-EM (0.25, 0.5, 1, 2 mg/mL).  $\text{CF}_3\text{SO}_3\text{Na}$  ( $\delta$ : -78.7 ppm) was added directly as an internal reference. The relative peak integral of  $\text{CF}_3\text{SO}_3\text{Na}$  for each group was normalized as 1.0, and the other relative peak integrals of Neu@PFC ( $\delta$ : -91.9 ppm) were scaled accordingly.

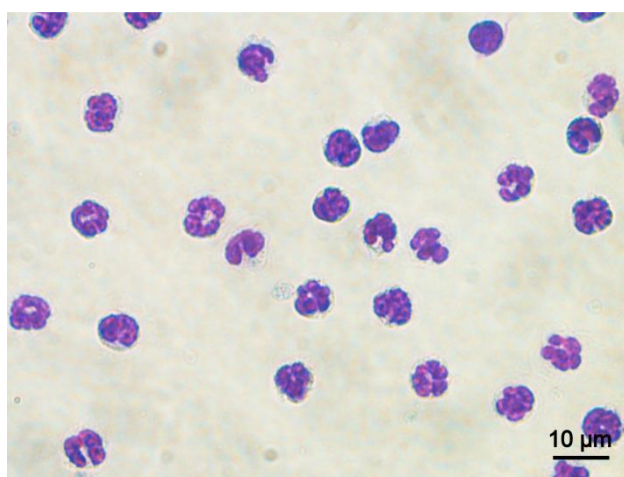


Figure S10. Wright-Giemsa staining of Neu@PFC.

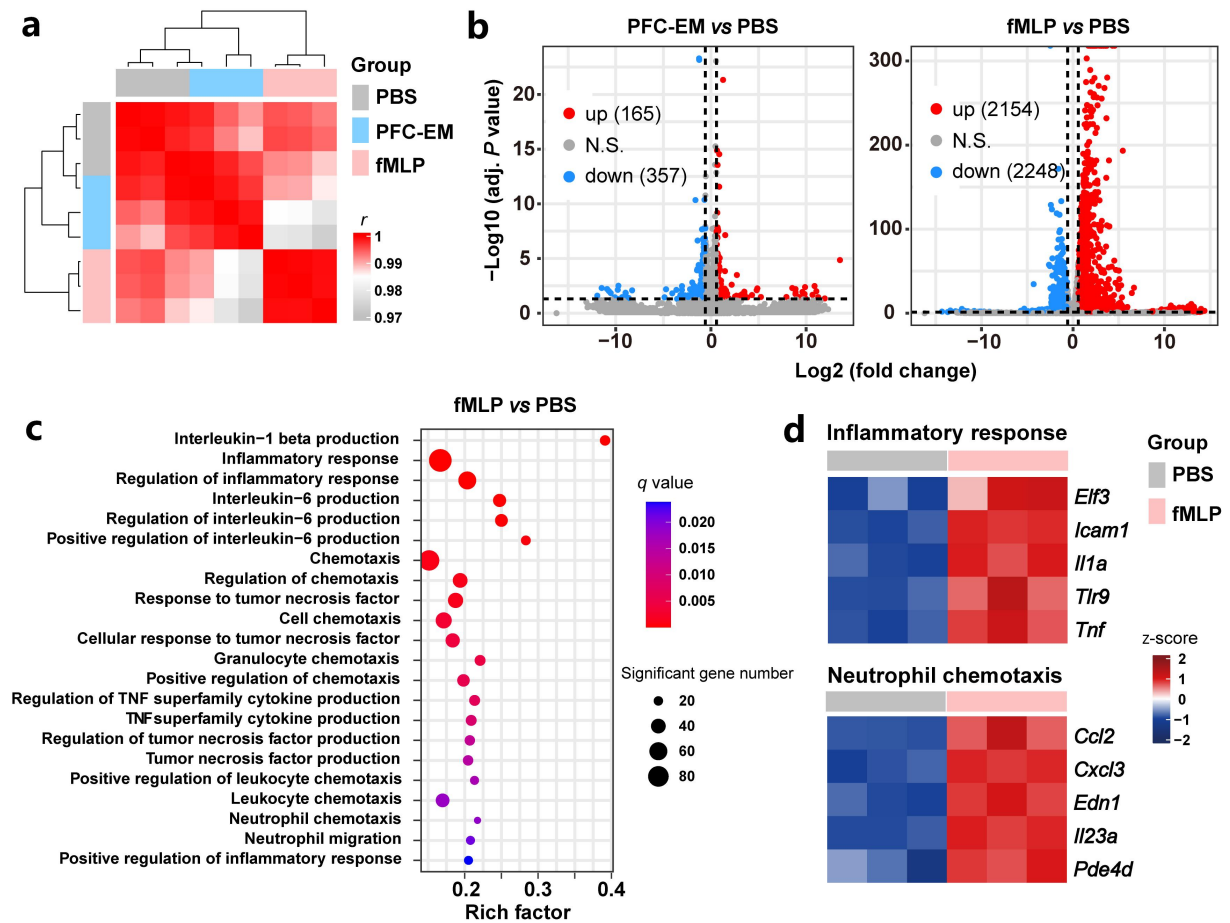


Figure S11. Transcriptomic analysis of neutrophils subjected to different treatments. (a) Correlation heatmap of neutrophils after incubation with PFC-EM, fMLP and PBS as control. (b) Volcano plots of differentially expressed genes (DEGs) in neutrophils of PFC-EM group and fMLP group, respectively. (c) Gene ontology (GO) analysis of upregulated DEGs in the fMLP group. (d) Expression heatmap of representative DEGs in inflammatory response and neutrophil chemotaxis pathways in neutrophils after incubation with fMLP or PBS.



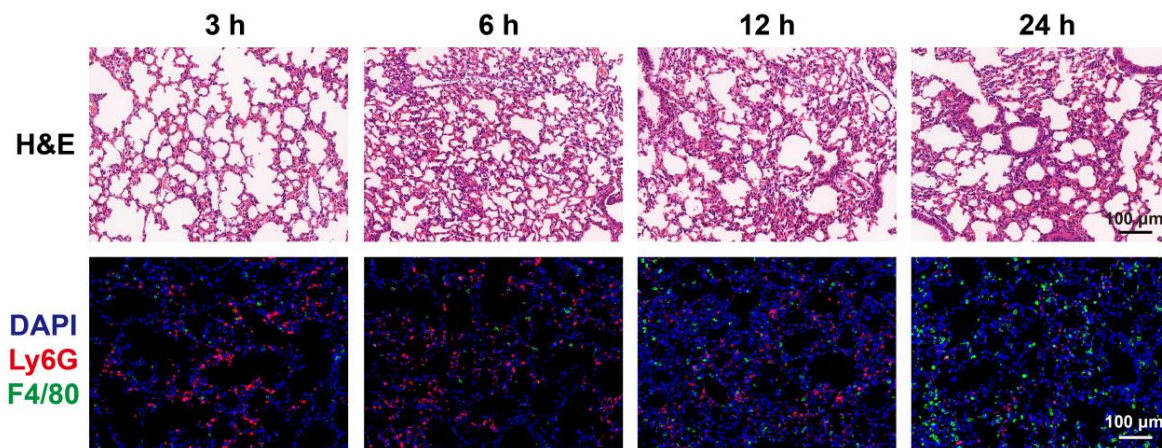


Figure S12. Representative H&E and immunofluorescence staining images of LPS (6  $\mu\text{g/g}$ , 100  $\mu\text{L}$ ) challenged lungs for different times (3, 6, 12, 24 hours). The alveolar inflammatory cell exudation and infiltration were investigated by fluorescently marking neutrophils with anti-Ly6G antibody (red) and macrophages with anti-F4/80 antibody (green), respectively. LPS-challenged ALI mice demonstrated significant pathological changes such as alveolar wall thickening, diffuse cellular injury, and dramatic neutrophil infiltration. Neutrophils rapidly infiltrate the injured lung tissue within 3-12 hours after modeling. By the 24-hour mark, neutrophils were gradually cleared from the lung tissue through phagocytosis by infiltrated macrophages.

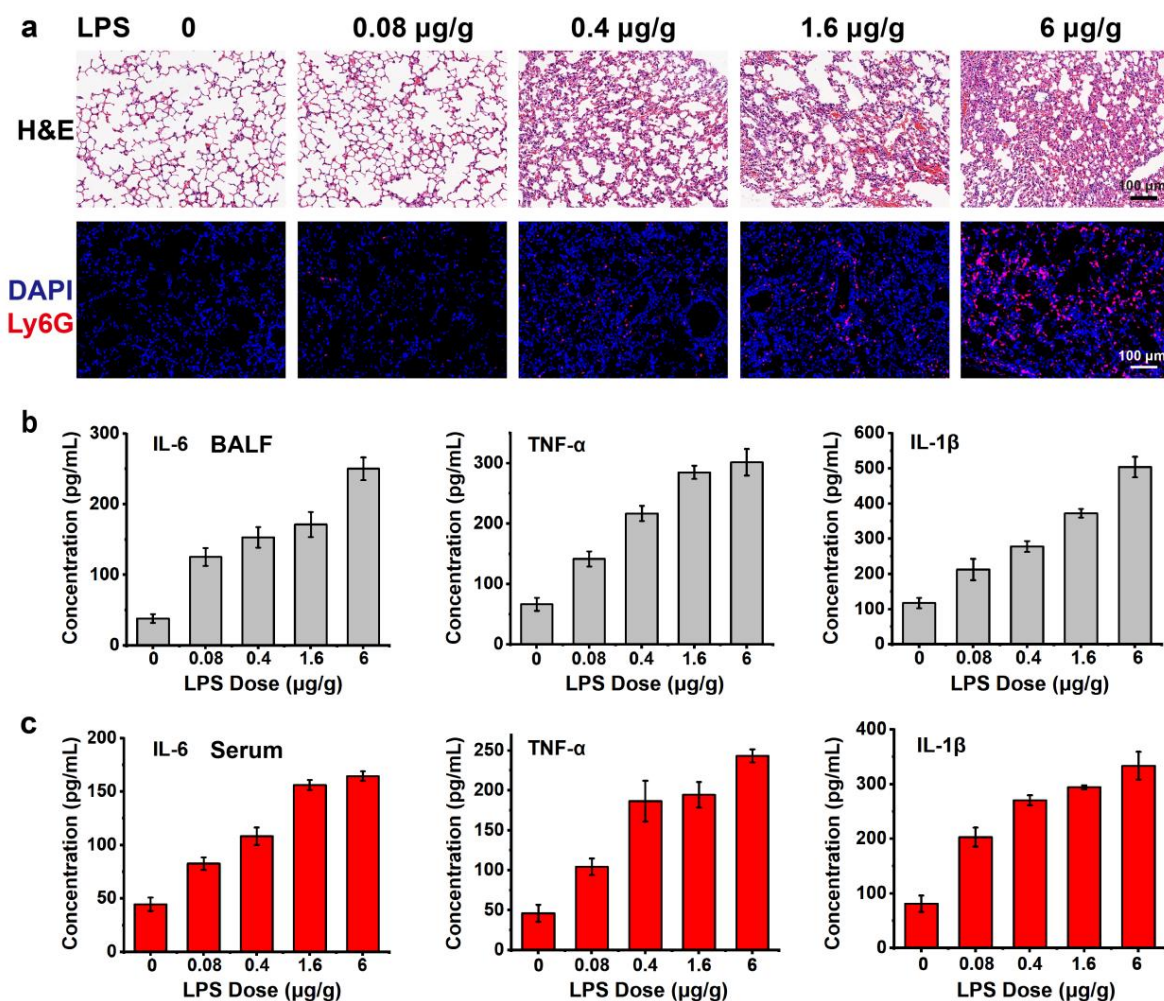


Figure S13. (a) Representative H&E and immunofluorescence staining images of lung tissues from mice after 12 hours of *i.t.* administration with PBS and LPS (0.08, 0.4, 1.6, 6  $\mu\text{g/g}$ ). The expression level of inflammatory cytokines TNF- $\alpha$ , IL-6 and IL-1 $\beta$  in BALF (b) and serum (c) were detected by ELISA. Based on the histomorphology, it was observed that the alveolar walls in the lung tissues of normal mice remained intact. However, lungs challenged with LPS exhibited significant pathological alterations such as alveolar collapse, interstitial edema, and neutrophil infiltration. Moreover, the higher the concentration of LPS instillation, the more severe the lung injury. Additionally, the expression levels of pro-inflammatory cytokines, including TNF- $\alpha$ , IL-6, and IL-1 $\beta$ , were significantly elevated in both the BALF and serum of LPS-challenged mice. (Mean  $\pm$  S.D.,  $n = 3$ ).

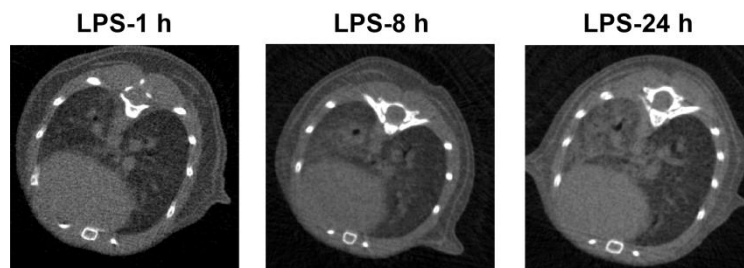


Figure S14. Transverse CT images of LPS (6  $\mu\text{g/g}$ ) induced ALI mice for 1, 8 and 24 hours.

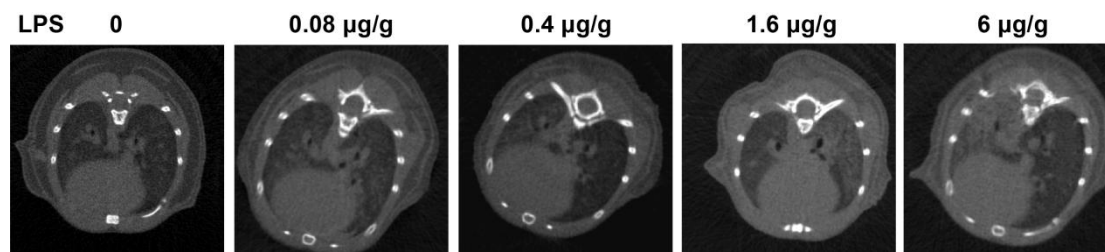


Figure S15. Transverse CT images of normal and ALI mice after 12 hours of *i.t.* administration with PBS and LPS (0.08, 0.4, 1.6, 6  $\mu\text{g/g}$ ).

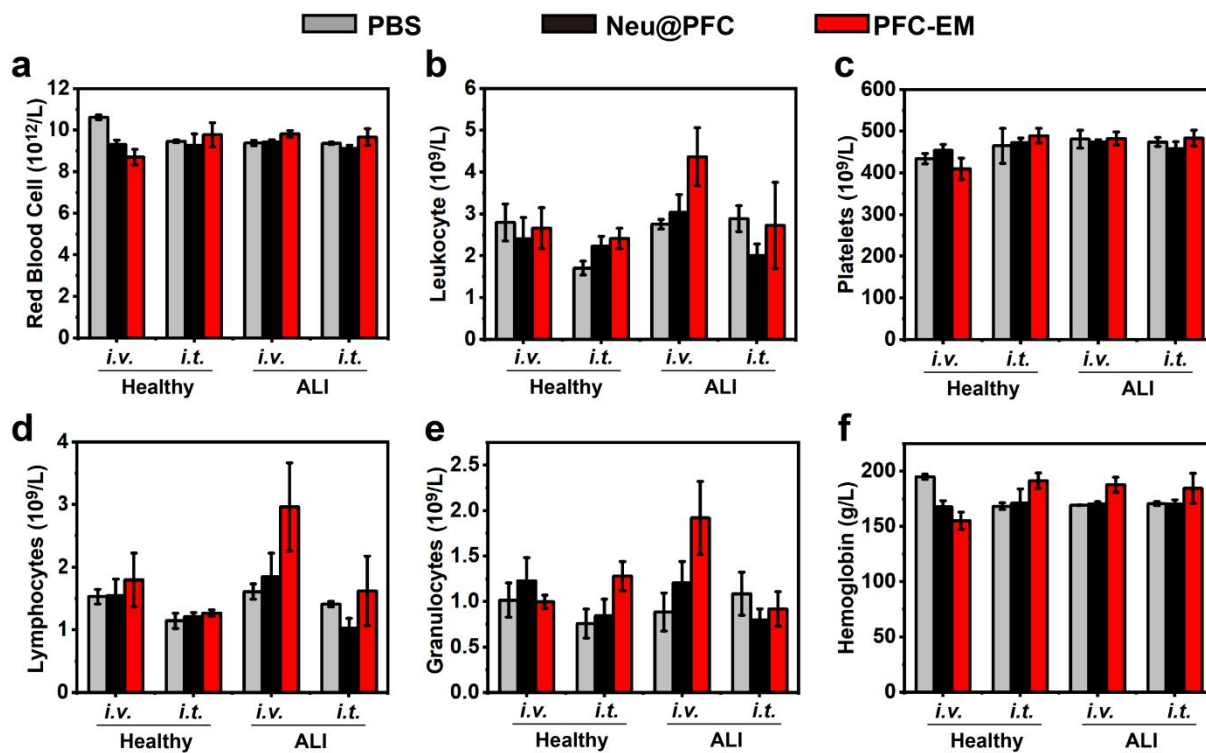


Figure S16. The quantities of (a) red blood cells, (b) leukocytes, (c) platelets, (d) lymphocytes, (e) granulocytes, and (f) hemoglobin in the blood were measured on the healthy and ALI mice following *i.v.* and *i.t.* administration of PBS, Neu@PFC and PFC-EM for 12 hours. (Mean  $\pm$  S.D., n = 3).

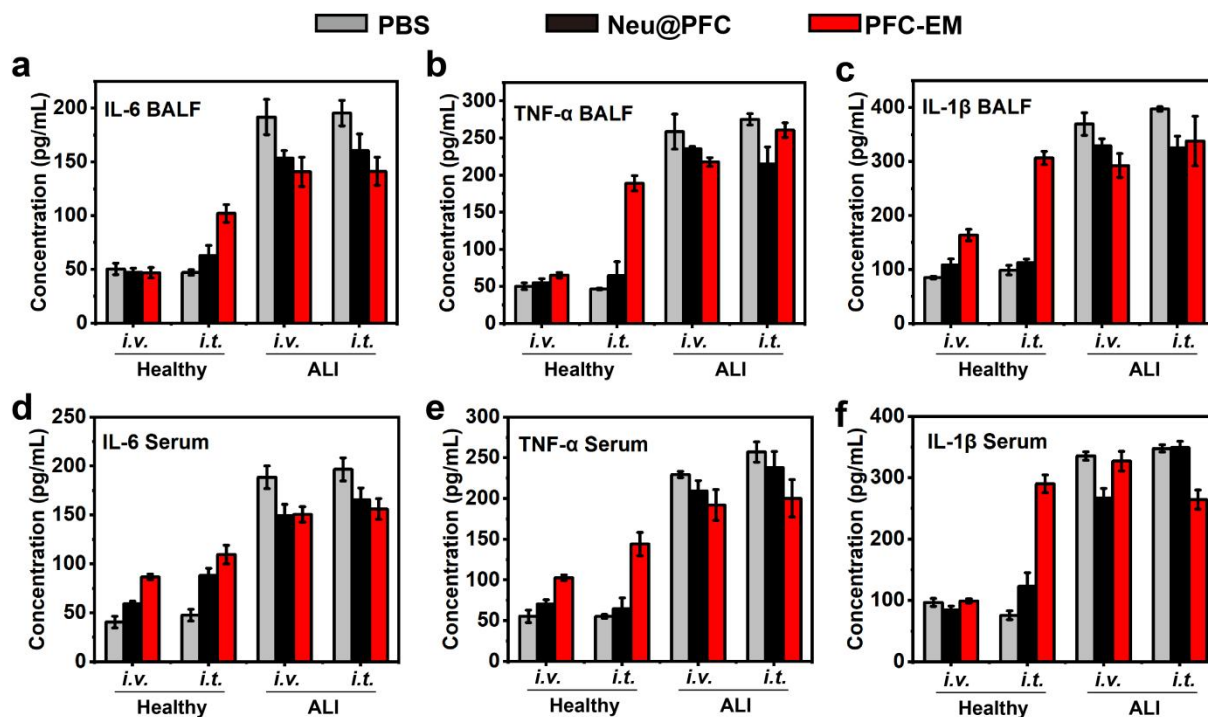


Figure S17. Evaluation of IL-6, TNF- $\alpha$ , and IL-1 $\beta$  levels in serum and BALF following *i.v.* and *i.t.* administration of PBS, Neu@PFC and PFC-EM for 12 hours. (Mean  $\pm$  S.D., n = 3).

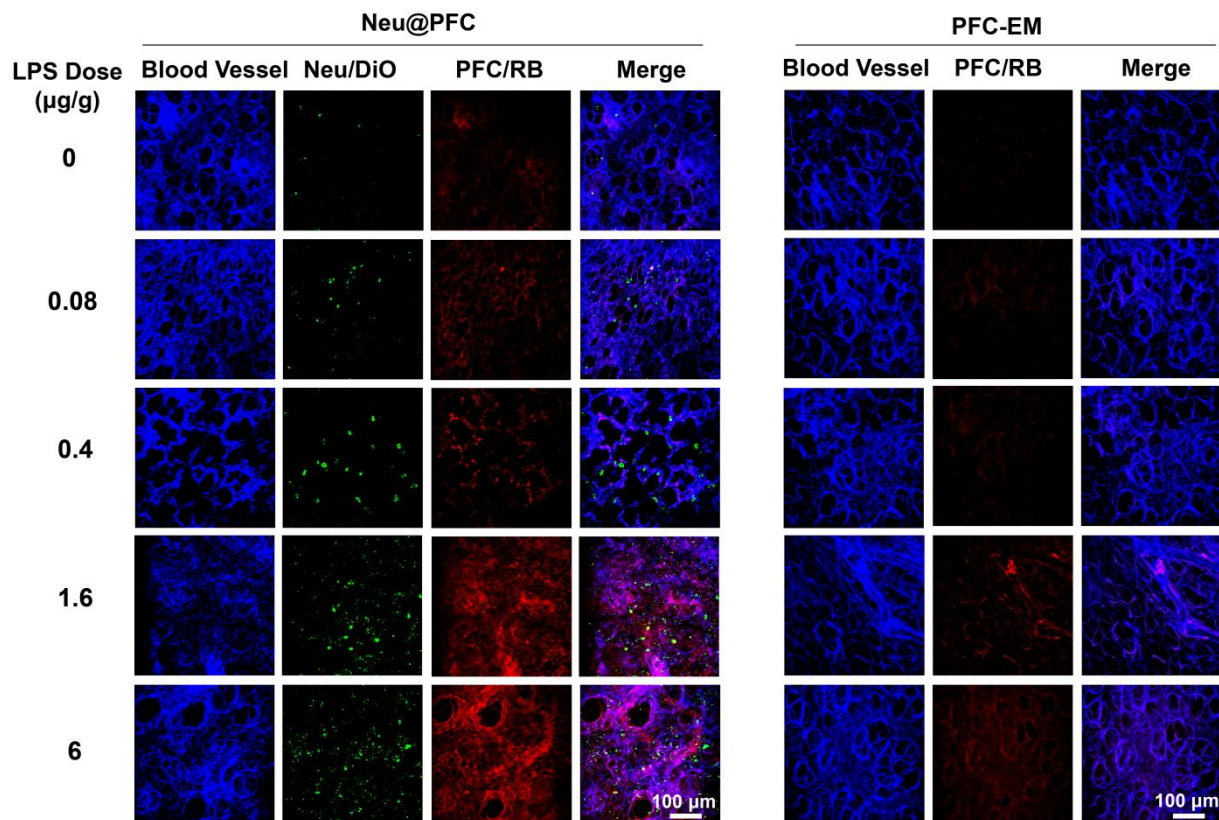


Figure S18. The IVM lung imaging of mice after *i.v.* administration of Neu@PFC and PFC-EM to different groups. Staining depicts DiO labeled neutrophils (green), Rhodamine-B labeled PFC-EM (red), and evance blue labeled vasculature (blue).

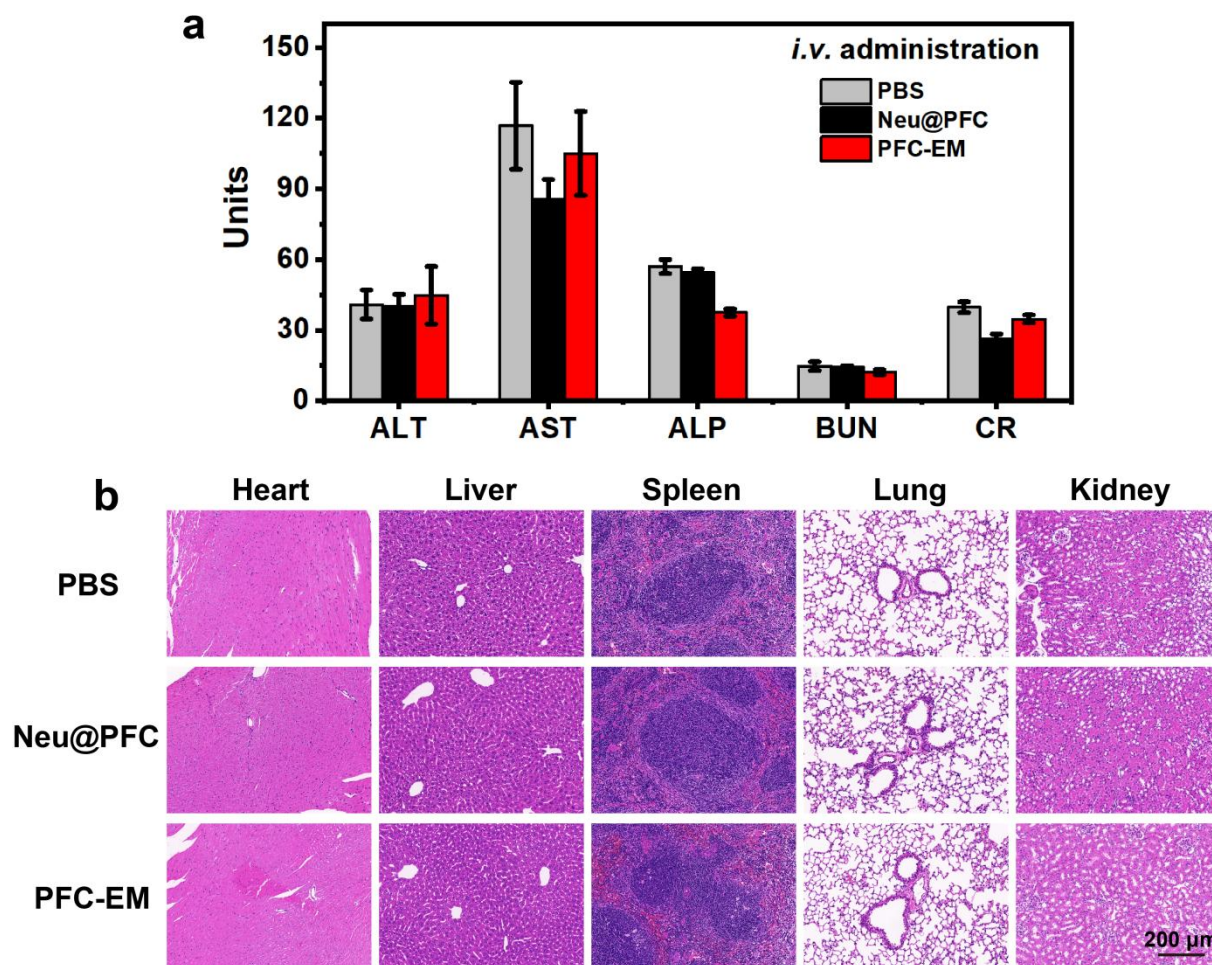


Figure S19. *In vivo* biocompatibility evaluation of PFC-EM and Neu@PFC after *i.v.* administration through the tail vein. (a) Blood biochemical analysis. (Mean  $\pm$  S.D.,  $n = 3$ ). (b) Histochemistry analysis of mice's heart, liver, spleen, lungs, and kidneys after *i.v.* administration of PBS, PFC-EM and Neu@PFC.

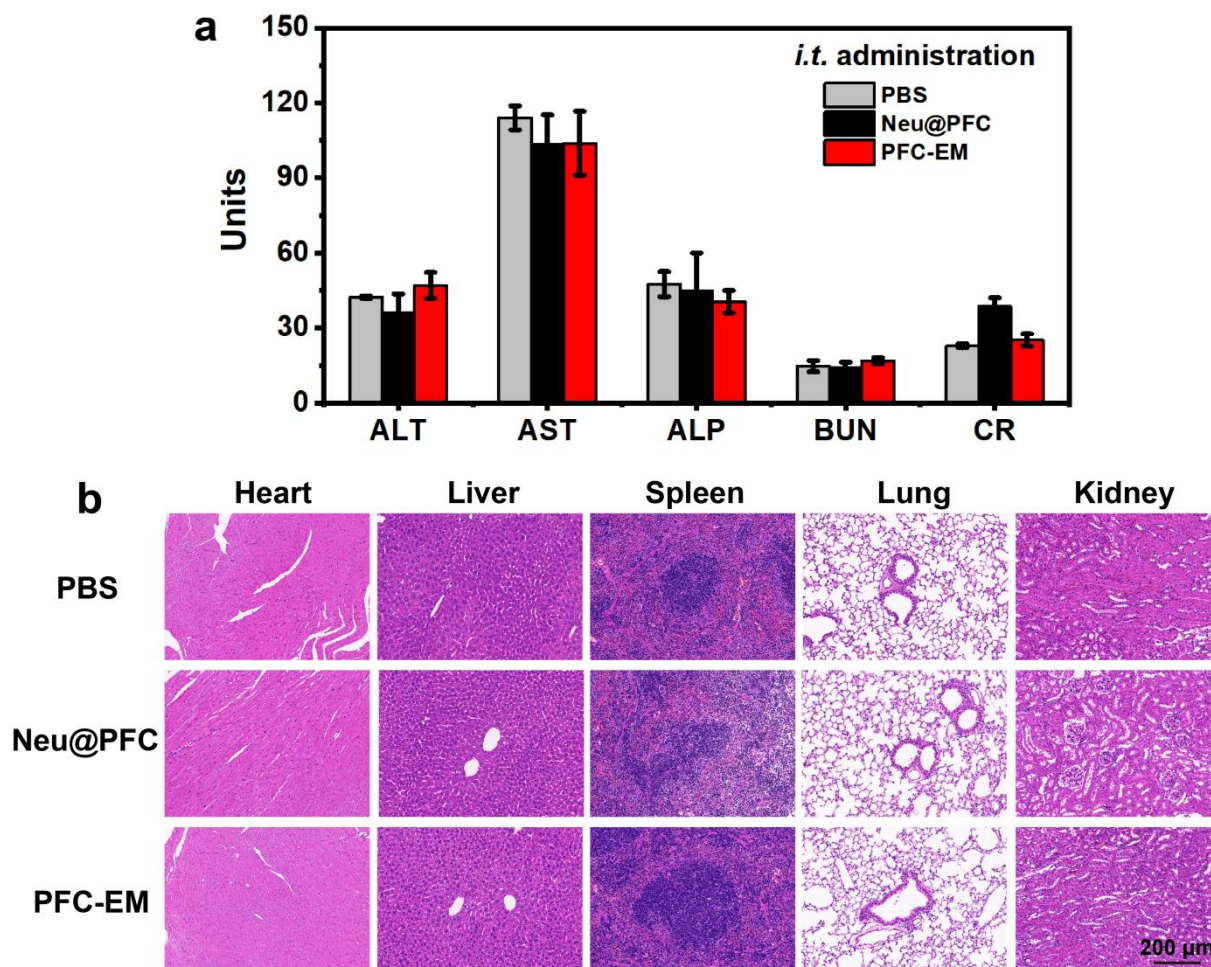


Figure S20. *In vivo* biocompatibility evaluation of PFC-EM and Neu@PFC after *i.t.* administration. (a) Blood biochemical analysis. (Mean  $\pm$  S.D.,  $n = 3$ ). (b) Histochemistry analysis of mice's heart, liver, spleen, lungs, and kidneys after *i.t.* administration of PBS, PFC-EM and Neu@PFC.

## Reference

- [1] U. Flögel, S. Temme, C. Jacoby, T. Oerther, P. Keul, V. Flocke, X. W. Wang, F. Bönner, F. Nienhaus, K. Peter, J. Schrader, M. Grandoch, M. Kelm, B. Levkau, *Nat. Commun.* **2021**, *12*, 5847.
- [2] J. W. Xue, Z. K. Zhao, L. Zhang, L. J. Xue, S. Y. Shen, Y. J. Wen, Z. Y. Wei, L. Wang, L. Y. Kong, H. B. Sun, Q. N. Ping, R. Mo, C. Zhang, *Nat. Nanotechnol.* **2017**, *12*, 692-700.